Mechanism of Product Specificity of AdoMet Methylation Catalyzed by Lysine Methyltransferases: Transcriptional Factor p53 Methylation by Histone Lysine Methyltransferase SET7/9[†]

Xiaodong Zhang and Thomas C. Bruice*

Department of Chemistry and Biochemistry, University of California, Santa Barbara, California 93106

Received December 3, 2007

ABSTRACT: The catalysis by SET7/9 histone lysine methyltransferase of AdoMet N-methylation of the transcriptional factor p53-Lys4-NH_2 has been investigated with particular attention paid to the means of product specificity. After formation of the SET7/9•p53-Lys4-NH_3^+•AdoMet complex, the following events occur: (i) the appearance of a water channel, (ii) a depronation of p53-Lys4-NH_3^+ via this water channel into the aqueous solvent, and (iii) AdoMet methylation of p53-Lys4-NH_2 to form p53-Lys4-N(Me)H_2^+. The formation of a water channel does not occur on formation of the SET7/9•p53-Lys4-NH_3^+, SET7/9•p53-Lys4-N(Me)H_2^+•AdoHcy, or SET7/9•p53-Lys4-N(Me)H_2^+•AdoMet complex. Without a water channel, the substrate p53-Lys4-N(Me)H is not available because the proton dissociation p53-Lys4-N(Me)H_2^+ → p53-Lys4-N(Me)H + H^+ does not occur. The lack of formation of a water channel is due to the positioning of the methyl substituent of the SET7/9•p53-Lys4-N(Me)H_2^+•AdoMet complex. By quantum mechanics/molecular mechanics, the computed free energy barrier of the methyl transfer reaction [p53-Lys4-NH_2 + AdoMet → p53-Lys4-N(Me)H_2^+ + AdoHcy] in the SET7/9 complex is $\Delta G^{\ddagger} = 20.1 \pm 2.9$ kcal/mol. This $\Delta G^{\ddagger}$ is in agreement with the value of 20.9 kcal/mol calculated from the experimental rate constant (1.2 ± 0.1 min^{-1}). Our bond-order computations establish that the methyl transfer reaction in protein lysine methyltransferases occurs via a linear S_N2 associative reaction with bond making of ~50%.

The structure of DNA in eukaryotic cells is known as chromatin. The methylation by protein lysine enzymes (PKMT), in particular histone lysine methyltransferase, is an important reaction in the regulation of chromatin structure (*1*). All but one (*2, 3*) of the known PKMTs (*4–16*) have a SET domain (*17, 18*). SET domain possesses a novel fold and use adjacent domains for both structural stabilization and the completion of the active site. The cofactor *S*-adenosylmethionine (AdoMet)[1] and substrate bind at two adjacent sites of the conserved SET domain. The side chain of the target lysine approaches the AdoMet methyl which will be transferred through a channel that passes thorough the middle of this SET domain.

PKMTs are capable of transferring one, two, or three methyl groups from AdoMet to the target lysine residue (Scheme 1). There are three reaction steps in each methyl transfer. They are (i) combination of enzyme•Lys-NH_3^+ with AdoMet, (ii) formation of a water channel and the ionization of enzyme-bound Lys-NH_3^+ to provide enzyme•Lys-NH_2•AdoMet, and (iii) methyl transfer providing enzyme•Lys-N(Me)H_2^+•AdoHcy and the dissociation of AdoHcy. The key is how PKMTs perform processively the multiple methyl transfer steps because different mono-, di-, and trimethylation products (known as product specificity) have different influences on chromatin structure and transcription (*9*). To elucidate the processivity and multiplicity of the methyl transfer reactions, an absolutely conserved tyrosine (e.g., Tyr335 in SET7/9, Tyr287 in LSMT, Tyr336 in SET8, and Tyr105 in vSET) in SET domain enzymes was proposed to, as a Tyr-O^-, be the general base to deprotonate the positively charged lysine (*7*). This proposal, based on a single residue at the active site, could not reasonably explain the processivity of deprotonations of the mono- or dimethylated lysine because the pK_a of this Tyr-OH is greater than 13.0 (*22*). Xiao et al. (*10*) have proposed that the bulk solvent might play an important role in dissociation of the proton of the positively charged (methylated) lysine. This proposal seems unlikely because the reactants are enclosed at the active site and not subjected to solvent encroachment. Dirk et al. (*19*) suggested that a water molecule in the active site of PKMTs could be the proton acceptor. This is unlikely since H_3O^+ is a stronger acid than Lys-CH_2-NH_3^+.

Recently, SET7/9 was found to monomethylate transcriptional factor p53 with the sequence LKS**K**KGQSTY. In the study presented here, we employ hybrid QM/MM and MD simulations to investigate the mechanism of this reaction and the reason that SET7/9 only monomethylates p53 as a

[†] T.C.B. expresses deep gratitude to the National Institutes of Health for 52 years of continuous support ending August 2007 with a study section turn away of NIH 5R37DK9171-44.

* To whom correspondence should be addressed. E-mail: tcbruice@chem.ucsb.edu. Telephone: (805) 893-2044. Fax: (805) 893-2229.

[1] Abbreviations: SET7/9, histone lysine methyltransferase; AdoMet, *S*-adenosylmethionine; AdoHcy, *S*-adenosyl-L-homocysteine; MD, molecular dynamics; QM/MM, quantum mechanics/molecular mechanics; SCCDFTB, self-consistent-charge density-functional tight binding; CPR, conjugate peak refinement; TS, transition state.

10.1021/bi702370p CCC: $40.75
Published on Web 02/09/2008

Scheme 1

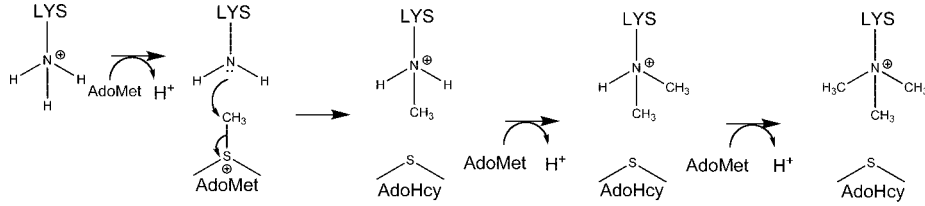

substrate. The results of our previous (*20–22*) and current studies provide a definitive determination of the mechanism for the product specificity in protein lysine methyltransferase enzyme catalysis.

MATERIALS AND METHODS

The initial structure of the SET7/9·p53-Lys4·AdoMet complex was built from the X-ray structure [PDB entry 1XQH (*23*)] of the SET7/9 enzyme with AdoHcy and the methylated Lys [Lys4-N(Me)] peptide substrate. The methyl group of enzyme-bound AdoMet was built on the basis of the SET7/9·p53-MeLys4·AdoHcy structure.

A water [TIP3P (*24*)] sphere with a 25 Å radius was centered at the AdoMet cofactor. Hydrogen atoms were added to the crystal structure using the HBUILD module implemented in CHARMM (*25*) (version 31b1), and CHARMM31 force field parameters (*26, 27*) were employed. A spherical boundary potential (*28*) for a 25 Å radius was used to prevent the water from "evaporating" from the surface. Each complex, including SET7/9·p53-Lys4-NH_3^+, SET7/9·p53-Lys4-NH_3^+·AdoMet, SET7/9·p53-Lys4-NH_2·AdoMet, SET7/9·p53-Lys4-N(Me)-H_2^+·AdoHcy, SET7/9·p53-Lys4-N(Me)H_2^+, SET7/9·p53-Lys4-N(Me)H_2^+·AdoMet, and SET7/9·p53-Lys4-N(Me)H·AdoMet, was minimized by the adopted basis Newton−Rasphon (ABNR) method until the gradient was less than 0.01 kcal mol^{-1} $Å^{-1}$ at the MM level. Stochastic boundary molecular dynamics (SBMD) (*29*) were carried out for 3.0 ns on each complex. An integration time step of 1 fs was used, with all the bonds involving hydrogen atoms constrained using SHAKE (*30*). The presence of a water channel is established by determining the distances between the hydrogen and oxygen atoms of the continuous water molecules. A distance of 1.85 Å supports a water channel. The average densities of the water molecules in a water channel confirm the formation of a water channel. The pK_a of Lys-NH_3^+ in each of 10 snapshots is estimated using the PBEQ (*31, 32*) module implemented in CHARMM, with 4.0 as the dielectric constant of the protein at the MM level. For the pK_a calculations, the atomic radii are taken from ref *33* and the partial charge of the neutral lysine residue is from ref *34*.

Fifteen snapshots of each SET7/9·p53-Lys4-NH_2·AdoMet and SET7/9·p53-Lys4-N(Me)H·AdoMet complex were picked up with the interval of 200 ps. Each of the 15 snapshots was minimized by QM/MM methods [QM = SCCDFTB (*35, 36*), self-consistent-charge density-functional tight binding] until the gradient was less than 0.01 kcal mol^{-1} $Å^{-1}$, which led to an optimized structure of the reactant. In the QM/MM calculations, the QM region included the -CH_2-S^+(Me)-CH_2- part of the AdoMet cofactor, and the side chain of the neutral lysine 4 in the peptide substrate (Lys4-NH_2) [or neutral monomethylated lysine 4, Lys4-N(Me)H]. Link atoms were introduced to saturate the valence of the QM boundary atoms.

Adiabatic mapping calculations at the SCCDFTB/MM level were carried out using the two-dimensional potential energy surface (PES). The two-dimensional reaction coordinates were the N_ϵ(Lys4)−C_γ(AdoMet) and C_γ(AdoMet)−S_δ(AdoMet) distances. The transition states were obtained by using conjugate peak refinement (CPR) (*37*) implemented in the Trajectory Refinement and Kinematics module of CHARMM, and normal-mode analysis provided only one imaginary frequency for characterizing the transition state. SCCDFTB for this methyl transfer reaction (*22*) is validated as compared with the B3LYP/6-31G*//MM calculations (*38*). The Wiberg bond-order analysis (*39*) of the bond making and breaking in the SCCDFTB/MM-determined transition states was carried out using B3LYP/6-31+G(d,p) [Gaussian (*40*)] in the gas phase.

The free energies were obtained using the equation $\Delta G = \Delta E + \Delta E_{Ther} + \Delta(ZPE) - T\Delta S$ (*41*). To obtain more quantitative free energy barriers, single-point computations at the MP2/6-31+G(d,p)//MM (Gamess-US version, June 22, 2002) (*42*) level were carried out. The potential energy (ΔE) was provided by QM/MM. The thermal energy (ΔE_{Ther}) could be expressed as $\Delta E_{Ther} = \Delta E_{Trans} + \Delta E_{Rot} + \Delta E_{Vib}$. The vibrational contributions [Δ(ZPE), ΔE_{vib}, and $-T\Delta S$] were determined with harmonic approximation at 298 K by normal-mode analysis. Because the thermal energies and entropies from the transition motion (E_{Trans}) and rotation motion (E_{Rot}) are linear with temperature according to their corresponding statistical equations, their contributions to the reaction barrier (or reaction energy) should be approximately zero for an enzymatic reaction at constant temperature.

The residues within 16 Å of AdoMet in all species (reactant, transition state, and product) were included in normal-mode analysis to provide $3N - 6$ frequencies, which were employed to calculate the zero-point energy, the thermal vibrational energy, and the entropy. (N is the number of atoms within the reduced regions; residues beyond that were fixed in the vibrational calculations.)

A perturbation analysis similar to that in refs *43* and *44* was performed to analyze the influence of individual residue on the reaction barrier. Because the electrostatic contribution to the reaction barrier dominates that from van der Waals interactions, the perturbation treatment is restricted to the former. The electrostatic contribution ($\Delta\Delta E^{\ddagger}$) of a residue to the reaction barrier is defined as the difference between the potential energy barrier for a residue with no charge and that with its normal charge. Due to the extensive QM/MM calculations required, the analysis was carried out at the SCCDFTB/MM level.

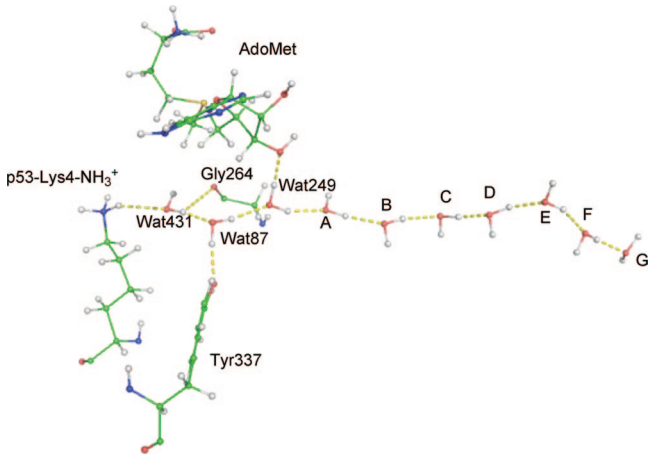

FIGURE 1: Snapshot of a water channel created upon formation of the SET7/9•p53-Lys4-NH_3^+•AdoMet complex. The solvent water molecules are designated A−G, and molecule G is on the surface of the water sphere with a 25 Å radius. The crystal water molecules are denoted Wat.

RESULTS AND DISCUSSION

Formation of the Neutral Substrate p53-Lys4-NH_2. Throughout our 3 ns study of MD simulations of SET7/9•p53-Lys4-NH_3^+•AdoMet, a water channel is positioned to allow proton transfer from p53-Lys4-NH_3^+ to the water solvent (Figure 1). The average densities (Table 1) of the hydrogen bonding between channel water (<1.85 Å) molecules confirm the formation of a channel of nine waters. Wat431 is hydrogen bonded to Lys4-NH_3^+ and becomes the starting point of a water channel (Figure 1). Wat431 could not be the proton acceptor by itself since H_3O^+ is a much stronger acid than Lys-NH_3^+. Examination of the environment around the water channel shows that there is no general base candidate. The PKMT selects the solvent molecules and the water molecules at the active site, forming a water channel for the proton from p53-Lys4-NH_3^+ to dissociate into the solvent. When a hydroxide ion is positioned at molecule A (Figure 1), there is no energy barrier for transfer of a proton from p53-Lys4-NH_3^+ through a water channel to HO^- at the QM/MM level [QM = both SCCDFTB and HF/6-31+G(d,p)]. Calculations (see Materials and Methods) establish that the average pK_a of p53-Lys4-NH_3^+ in the SET7/9•p53-Lys4-NH_3^+ complex is 11.3 ± 1.2. After the cofactor AdoMet enters, the average pK_a of p53-Lys4-NH_3^+ in the SET7/9•p53-Lys4-NH_3^+•AdoMet complex decreases to 5.8 ± 1.4. This decrease is due to the electrostatic interaction of positive charges of adjacent Lys-NH_3^+ and $^+$AdoMet. Because the concentration of HO^- at the optimal pH of 8.0 is 10^{-6}, the activation energy barrier for proton dissociation would be 8.4 kcal/mol.

Energetics for the First Methyl Transfer Reaction. The reaction coordinates for the first methyl transfer reaction [SET7/9•p53-Lys4-NH_2•AdoMet → SET7/9•p53-Lys4-N(Me)H_2^+•AdoHcy] are shown in Figure 2. The key geometric parameters at the ground state SET7/9•p53-Lys4-NH_2•AdoMet are listed in Scheme 2.

Normal-mode analysis characterizes the transition state of the first methylation step (TS-M) with only one imaginary frequency of 288 ± 66i cm^{-1}. The key geometric parameters of TS-M are shown in Scheme 3. The linear S_δ(AdoMet)···C_γ(AdoMet)···N_ϵ(p53-Lys4-NH_2) configuration (Scheme 3) in the ground state favors a concerted in line S_N2 mechanism (*45*). This feature is shared by the transition states of the first methyl transfer step catalyzed by LSMT and vSET. The Wiberg bond order analysis (Scheme 3) of N_ϵ(p53-Lys4)···C_γ(AdoMet) and C_γ(AdoMet)···S_δ(AdoMet) bonds at the transition state (TS-M) of the first methyl transfer step is characterized as 54% associative and 46% dissociative (*45*). The average free energy barrier of the methyl transfer reaction is determined with the equation $\Delta G^\ddagger = \Delta E^\ddagger + \Delta(\mathrm{ZPE})^\ddagger - T\Delta S^\ddagger + \Delta E_{vib}{}^\ddagger = 19.6 + 0.4 + 1.7 - 1.6 = 20.1$ kcal/mol (Figure 2) and is in agreement with the free energy barrier (20.9 kcal/mol) calculated from the experimental rate constant (1.2 ± 0.1 min^{-1}) (*46*). The deviations of $\Delta G^\ddagger$, $\Delta E^\ddagger$, $\Delta(\mathrm{ZPE})^\ddagger$, $T\Delta S^\ddagger$, and $\Delta E_{vib}{}^\ddagger$ are ±2.9, ±0.5, ±0.4, ±1.1, and ±0.3 kcal/mol, respectively. Also, compared with the calculated free energy (30.9 ± 0.2 kcal/mol) (*47*) of the corresponding methyl transfer reaction in aqueous solution, the enzyme reduces the barrier by 10.8 kcal/mol. This indicates that enzyme enhances this methyl transfer reaction by ~10^8-fold.

The enzyme-catalyzed methyl transfer reaction is calculated to be exergonic overall: $\Delta G^\circ = \Delta E^\circ + \Delta(\mathrm{ZPE})^\circ - T\Delta S^\circ + \Delta E_{vib}{}^\circ = -15.6 + 0.8 + 1.1 - 0.5 = -14.2$ kcal/mol (Figure 2). The deviation in ΔG° is ±0.3 kcal/mol. The key geometric parameters of the product are listed in Scheme 4. On comparison with the immediate product of the first methyl transfer reaction by LSMT (153 ± 6°) (*20*) and vSET (153 ± 12°) (*22*), the slightly less linear N(p53-Lys4-N(Me)H_2^+)−C_γ(AdoHcy)···S_δ(AdoHcy) (168 ± 8°) configuration (Scheme 4) is somewhat less favorable to reaction.

Perturbation Analysis (43, 44) of the Contribution from Electrostatic Interaction. The results (Table 2) of the perturbation analysis (see Materials and Methods) for the methyl transfer step involving the different peptide substrate p53 and peptide substrate denoted by WT [substrate sequence, ART**K**QTARKT] by SET7/9 indicate that the dominant and favorable effects of Thr245, Lys294, Asp338, Asp270, and Asp306 decrease the activation energy barrier compared with that in aqueous solution and in the gas phase model. These residues stabilize the transition state. The residues with unfavorable and dominant contributions to the reaction barrier include Glu228, His293, Lys317, Glu330, Leu1^{p53}/Ala1^{WT}, Glu220, Glu279, and Asn265. These residues stabilize the reactant state. Lys5 in p53 has an unfavorable contribution; Gly6 in p53 has a favorable contribution to the reaction barrier, while the corresponding residues in WT make smaller contributions to the reaction barrier.

A Water Channel Determines the Product Specificity. In 3 ns MD simulations of the product, SET7/9•p53-Lys4-N(Me)H_2^+•AdoHcy as well as SET7/9•p53-Lys4-N(Me)H_2^+ do not show formation of a water channel. Most importantly, MD simulations of SET7/9•p53-Lys4-N(Me)H_2^+•AdoMet do not support proton dissociation of p53-Lys4-N(Me)H_2^+ since a water channel is not formed. The conformations of active site-bound p53-Lys4-NH_3^+•AdoMet and p53-Lys4-N(Me)H_2^+•AdoMet are shown in panels A and B of Figure 3, respectively. Inspection of Figure 3 establishes that the methyl group of p53-Lys4-N(Me)H_2^+ takes the position of the proton of p53-Lys4-NH_3^+ that forms a water channel. Thus, the dissociation of a proton from p53-Lys4-N(Me)H_2^+ does not occur due to the methyl substituent preventing water channel formation so that the neutral substrate p53-Lys4-

Table 1: Average Densities (in atoms per cubic angstrom) of the Water Molecules at the Positions of the Water Channel (shown in Figure 1) during the MD Simulations of the SET7/9•p53-Lys4-NH_3^+•AdoMet Complex[a]

position	Wat431	Wat87	Wat249	A	B	C	D	E	F	G
density	0.006	0.008	0.012	0.017	0.021	0.026	0.030	0.030	0.027	0.022

[a] The solvent–water molecules are designated A−G, and molecule G is on the surface of the water sphere with a 25 Å radius. The crystal water molecules are designated by Wat.

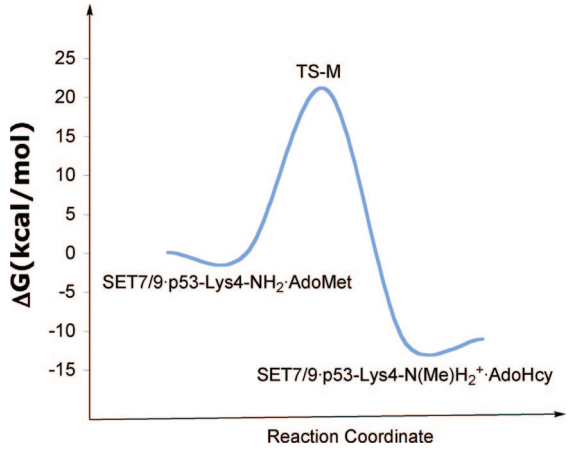

FIGURE 2: Schematic effective free energy surface for the methyl transfer reaction p53-Lys4-NH_2 + AdoMet → p53-Lys4-N(Me)H_2^+ + AdoHcy catalyzed by SET7/9.

Scheme 2

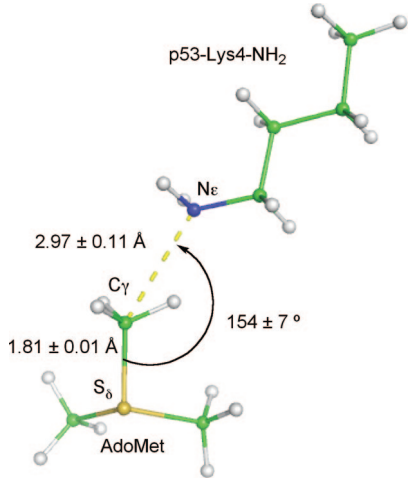

Scheme 3

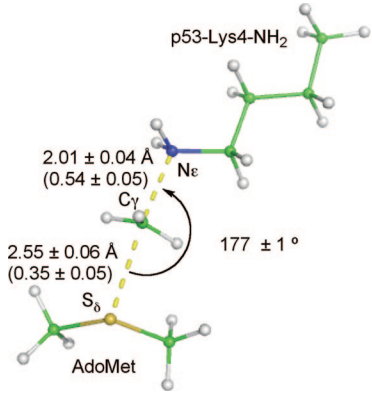

N(Me)H is not available. The hydrogen bond analysis (Table 3) and the calculated pK_a (13.8 ± 2.1) of p53-Lys4-N(Me)H_2^+ in SET7/9•p53-Lys4-N(Me)H_2^+•AdoMet confirms that dissociation of p53-Lys4-N(Me)H_2^+ is not possible.

Scheme 4

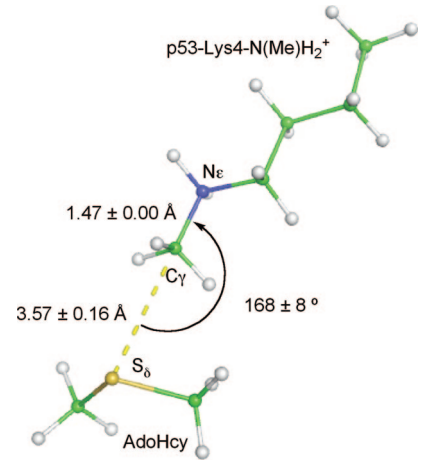

Table 2: Results of Perturbation Analysis for the Contributions ($\Delta\Delta E^{\ddagger}$ in kilocalories per mole) from Protein Residues to the Potential Energy Barrier for the First Methylation Step[a]

p53			WT		
residue	$\Delta\Delta E^{\ddagger}$	deviation	residue	$\Delta\Delta E^{\ddagger}$	deviation
Glu228	−6.07	0.81	Glu228	−3.49	0.50
His293	−4.12	0.59	His293	−1.94	0.41
Lys317	−3.82	0.49	Lys317	−2.06	0.48
$Lys5^S$	−2.90	0.52	$Lys5^S$	–	–
Glu330	−2.67	0.49	Glu330	−1.22	0.22
Leu1^S	−2.52	0.36	*Ala1*^{S}	−1.21	0.23
Glu220	−2.21	0.36	Glu220	−1.09	0.18
Glu279	−2.16	0.53	Glu279	−1.31	0.41
Asn265	−1.94	0.60	Asn265	−1.34	0.45
Asp306	1.90	0.18	Asp306	1.02	0.18
Asp270	2.10	0.23	Asp270	1.02	0.22
Asp338	2.21	0.20	Asp338	1.15	0.26
Glu271	2.31	0.34	Glu271	–	–
Lys294	3.48	0.42	Lys294	2.40	0.35
$Gly6^S$	3.53	0.38	$Gly6^S$	–	–
Tyr245	3.66	0.59	Tyr245	1.50	0.69

[a] The positive values indicate the favorable contributions that lower the barrier, and the negative values indicate the unfavorable contributions that increase the barrier. R is the distance from the α carbon of the residue to the center of the water sphere with a 25 Å radius. WT and p53 are the different peptide substrate with the different sequences (see the text). A superscript S denotes the residue from the peptide substrate.

Also, noting that methyl transfer is dependent upon the formation of a water channel is in accord with our previous studies of the LSMT (dimethyltransferase with a single lysine as a substrate), vSET (trimethyltransferase), and SET7/9 (monomethyltransferase) (*20–22*). Thus, the presence of a water channel is required by all SET domain enzymes for methyl transfer reactions.

Free Energy Profile for the "Supposed" Second Methyl Transfer Reaction. With the supposition that ionization of a proton has occurred to provide SET7/9•p53-Lys4-N(Me)H•AdoMet, the calculated average free energy barrier for the "second" methyl transfer step would be $\Delta G^{\ddagger} = \Delta E^{\ddagger} + \Delta(ZPE)^{\ddagger} - T\Delta S^{\ddagger} + \Delta E_{vib}^{\ddagger} = 23.2 + 1.0 + 2.1 - 0.8 = 25.6$

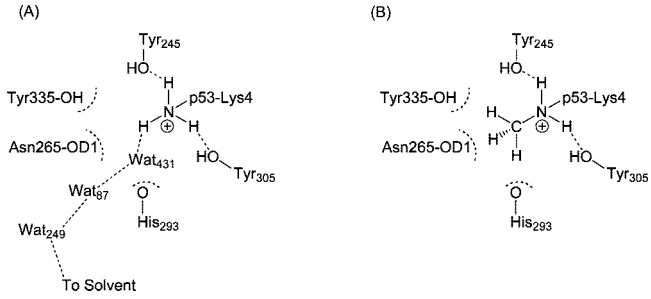

FIGURE 3: Schematic diagram of the position of an amine group at (A) p53-Lys4-NH_3^+•AdoMet in the SET7/9•p53-Lys4-NH_3^+•AdoMet and (B) p53-Lys4-N(Me)H_2^+ in complex SET7/9•p53-Lys4-N(Me)H_2^+•AdoMet.

Table 3: Average Occupancies of the Hydrogen Bond in the SET7/9•p53-Lys4-NH_3^+•AdoMet and SET7/9•p53-Lys4-N(Me)H_2^+•AdoMet Complexes

(methylated) lysine	HZ1	HZ2	HZ3
SET7/9•p53-Lys4-N(Me)H_2^+•AdoMet			
OH(Tyr245)	0.057	N/A[a]	0.739
OH(Tyr305)	0.648	N/A[a]	0.085
SET7/9•p53-Lys4-NH_3^+•AdoMet			
OH(Tyr245)	0.168	0.313	0.216
OH(Tyr305)	0.411	0.123	0.123

[a] Not available.

kcal/mol by QM/MM. The deviations of $\Delta G^{\ddagger}$, $\Delta E^{\ddagger}$, $\Delta(ZPE)^{\ddagger}$, $T\Delta S^{\ddagger}$, and $\Delta E_{vib}{}^{\ddagger}$ are ±3.3, ±3.0, ±0.5, ±1.1, and ±0.2 kcal/mol, respectively. In comparison with the average free energy barrier (20.1 kcal/mol) for the allowed methyl transfer step, this higher free energy barrier of 25.6 kcal/mol for the forbidden reaction [p53-Lys4-N(Me)H + AdoMet → p53-Lys4-$N(Me)_2H^+$ + AdoHcy] points to other factors which are unfavorable. The average S_δ(AdoMet)−C_γ(AdoMet)···N(p53-Lys4-N(Me)H) bond angle (142 ± 12°) at the reactant state SET7/9•p53-Lys4-N(Me)H•AdoMet is smaller than that in SET7/9•p53-Lys4-NH_2•AdoMet (154 ± 7°), and the C_γ(AdoMet)···N(p53-Lys4-N(Me)H) bond length in SET7/9•p53-Lys4-N(Me)H•AdoMet (3.53 ± 0.31 Å) is greater than that in SET7/9•p53-Lys4-NH_2•AdoMet (2.97 ± 0.11 Å). The SET7/9•p53-Lys4-N(Me)H•AdoMet conformations are not favorable for the second methyl transfer step. Zhang (*38*) and Guo (*48*) suggested that the near attack conformation (NAC) at the ground state determines the product specificities. We have shown just how this is established.

Normal-mode analysis shows that the transition state (TS-D) of the supposed step of methylation of SET7/9•p53-Lys4-N(Me)H•AdoMet has one and only one imaginary frequency of 318 ± 59i cm^{-1}. In TS-D, the N(p53-Lys4-N(Me)H)···C_γ(AdoMet) and C_γ(AdoMet)···S_δ(AdoMet) bond lengths are 2.56 ± 0.09 and 2.01 ± 0.05 Å, respectively, and the N(p53-Lys4-N(Me)H)···C_γ(AdoMet)···S_δ(AdoMet) bond angle is 174 ± 3°. Thus, the TS structures of both allowed and nonallowed methyl transfer steps (Scheme 3) are identical.

CONCLUSIONS

We have now employed p53 methylation by SET7/9 in the study of the product specificity in PKMTs. MD simulations show that a water channel appears only in the SET7/9•p53-Lys4-NH_3^+•AdoMet complex. The dissociation of the proton of p53-Lys4-NH_3^+ occurs via this water channel which is associated with a barrier of 8.4 kcal/mol at pH 8.0. A water channel does not form in SET7/9•p53-Lys4-N(Me)H_2^+•AdoHcy, SET7/9•p53-Lys4-NH_3^+, or SET7/9•p53-Lys4-N(Me)H_2^+•AdoMet. The conformation of the nitrogen substituent of p53-Lys4-CH_2N(Me)H_2^+ (Figure 3) determines the presence, or not, of the water channel and proton dissociation that creates the neutral p53-Lys4-N(Me)H substrate. Also, noting the dependence of methyl transfer occurring upon formation of a water channel in our previous studies of SET7/9, LSMT, and vSET (*20–22*) establishes a definitive mechanism. Our QM/MM calculated free energy barrier for the methyl transfer reaction [SET7/9•p53-Lys4-NH_2•AdoMet → SET7/9•p53-Lys4-N(Me)H_2^+•AdoHcy] is 20.1 ± 2.9 kcal/mol. This is in excellent agreement with the free energy barriers (20.9 kcal/mol) calculated from the experimental rate constants (1.2 ± 0.1 min^{-1}). The Wiberg bond order analysis and the structure at the transition state (Scheme 3) indicate that the p53 monomethylation by SET7/9 is a concerted linear S_N2 reaction.

ACKNOWLEDGMENT

Some of the calculations were performed at the National Center for Supercomputing Applications (University of Illinois, Urbana, IL).

REFERENCES

1. Strahl, B. D., and Allis, C. D. (2000) The language of covalent histone modifications. *Nature 403*, 41–45.
2. Feng, Q., Wang, H., Ng, H. H., Erdjument-Bromage, H., Tempst, P., Struhl, K., and Zhang, Y. (2002) Methylation of H3-lysine 79 is mediated by a new family of HMTases without a SET domain. *Curr. Biol. 12*, 1052–1058.
3. Min, J., Feng, Q., Li, Z. Z., Zhang, Y., and Xu, R. M. (2003) Structure of the catalytic domain of human DOT1L: A non-SET domain nucleosomal histone methyltransferase. *Cell 112*, 711–723.
4. Jacobs, S. A., Harp, J. M., Devarakonda, S., Kim, Y., Rastinejad, F., and Khorasanizadeh, S. (2002) The active site of the SET domain is constructed on a knot. *Nat. Struct. Biol. 9*, 833–838.
5. Xiao, B., Jing, C., Wilson, J. R., and Gamblin, S. J. (2003) SET Domain and Histone Metylation. *Curr. Opin. Struct. Biol. 13*, 699–705.
6. Xiao, B., Jing, C., Wilson, J. R., Walker, P. A., Vasisht, N., Kelly, G., Howell, S., Taylor, I. A., Blackburn, G. M., and Gamblin, S. J. (2003) Structure and Catalytic Mechanism of the Human Histone Methyltransferase SET 7/9. *Nature 421*, 652–656.
7. Kwon, T., Chang, J. H., Kwak, E., Lee, C. W., Joachimiak, A., Kim, Y. C., Lee, J., and Cho, Y. (2002) Mechanism of histone lysine methyl transfer revealed by the structure of SET7/9-AdoMet. *EMBO J. 22*, 292–303.
8. Couture, J., Collazo, E., Hauk, G., and Trievel, R. C. (2006) Structural Basis for the Methylation Site Specificity of SET7/9. *Nat. Struct. Mol. 13*, 140–146.
9. Couture, J., Collazo, E., Brunzelle, J. S., and Trievel, R. C. (2005) Structural and functional analysis of SET8, a histone H4 Lys-20 methyltransferase. *Genes Dev. 19*, 1455–1465.
10. Xiao, B., Jing, C., Kelly, G., Walker, P. A., Muskett, F. W., Frenkiel, T. A., Martin, S. R., Sarma, K., Reinberg, D., Gamblin, S. J., and Wilson, J. R. (2005) Specificity and mechanism of the histone methyltransferase Pr-Set7. *Genes Dev. 19*, 1444–1454.
11. Zhang, X., Yang, Z., Khan, S. I., Horton, J. R., Tamarn, H., Selker, E. U., and Cheng, X. (2003) Structural basis for the product specificity of histone lysine methyltransferase. *Mol. Cell 12*, 177–185.
12. Min, J., Zhang, X., Cheng, X., Grewal, S. I., and Xu, R. M. (2002) Structure of the SET domain histone lysine methyltransferase Clr4. *Nat. Struct. Biol. 9*, 828–832.
13. Qian, C., Wang, X., Manzur, K., Farooq, S. A., Zeng, L., Wang, R., and Zhou, M. (2006) Structural Insights of the Specificity and

Catalysis of a Viral Histone H3 Lysine 27 Methyltransferase. *J. Mol. Biol. 359*, 86–96.
14. Manzur, K. L., Farooq, A., Zeng, L., Plotnikova, O., Koch, A. W., Sachchildanand, and Zhou, M. M. (2003) A dimeric viral SET domain methyltransferase specific to Lys27 of histone H3. *Nat. Struct. Biol. 10*, 187–196.
15. Trivel, R. C., Flynn, E. M., Houtz, R. L., and Hurley, J. H. (2003) Mechanism of Multiple Lysine Methylation by the SET Domain Enzyme Rubisco LSMT. *Nat. Struct. Biol. 10*, 545–552.
16. Couture, J., Hauk, G., Thompson, M. J., Blackburn, G. M., and Trievel, R. C. (2006) Catalytic Roles for Carbon-Oxygen Hydrogen Bonding in SET Domain Lysine Methyltransferases. *J. Biol. Chem. 281*, 19280–19287.
17. Rea, S., Eisenhaber, F., O'Carroll, D., Strahl, B. D., Sun, Z., Schmid, M., Opravil, S., Mechtler, K., Ponting, C. P., Allis, C. D., and Jenuwein, T. (2000) Regulation of chromatin structure by site-specific histone H3 methyltransferases. *Nature 406*, 593–599.
18. Schultz, J., Milpetz, F., Bork, P., and Ponting, C. P. (1998) SMART, a simple modular architecture research tool: Identification of signaling domains. *Proc. Natl. Acad. Sci. U.S.A. 95*, 5857–5864.
19. Dirk, L. M. A., Flynn, E. M., Diwtzel, K., Couture, J., Trievel, R., and Houtz, R. L. (2007) Kinetic manifestion of processivity during multiple methylation catalyzed by SET domain protein methyltransferases. *Biochemistry 46*, 3905–3915.
20. Zhang, X. D., and Bruice, T. C. (2007) Catalytic Mechanism and Product Specificity of Rubisco Large Subunit Methyltransferase: QM/MM and MD Investigations. *Biochemistry 46*, 5505–5014.
21. Zhang, X.-D., and Bruice, T. C. (2007) Histone Lysine Methyltransferase SET7/9: Formation of a Water Channel Precedes Each Methyl Transfer. *Biochemistry 46*, 14838–14844.
22. Zhang, X.-D., and Bruice, T. C. (2007) A QM/MM Study on the Catalytic Mechanism and Product Specificity of Viral Histone Lysine Methyltransferase. *Biochemistry 46*, 9743–9751.
23. Chuikov, S., Kurash, J. K., Wilson, J. R., Xiao, B., Justin, N., Ivanov, G. S., Mckinney, K., Tempst, P., Prives, C., Gamblin, S. J., Barlev, N. A., and Reinberg, D. (2004) Regulation Of P53 Activity Through Lysine Methylation. *Nature 432*, 353.
24. Jorgensen, W. L., Chandrasekhar, J., Madura, J. D., Impey, R. W., and Klein, K. L. (1983) Comparison of simple potential functions for simulating liquid water. *J. Chem. Phys. 79*, 926–935.
25. Brooks, B. R., Bruccoleri, R. E., Olafson, B. D., States, D. J., Swaminathan, S., and Karplus, M. (1983) CHARMM: A Program for Macromolecular Energy, Minimization, and Dynamics Calculations. *J. Comput. Chem. 4*, 187–217.
26. MacKerell, A. D., Jr., Feig, M., and Brooks, C. L. (2004) Extending the treatment of backbone energetics in protein force fields: Limitations of gas-phase quantum mechanics in reproducing protein conformational distributions in molecular dynamics simulations. *J. Comput. Chem. 25*, 1400–1415.
27. MacKerell, A. D., Jr., Bashford, D., Bellott, M., Dunbrack, R. L., Jr., Evanseck, J. D., Field, M. J., Fischer, S., Gao, J., Guo, H., Ha, S., Joseph-McCarthy, D., Kuchnir, L., Kuczera, K., Lau, F. T. K., Mattos, C., Michnick, S., Ngo, T., Nguyen, D. T., Prodhom, B., Reiher, W. E., Roux, B., Schlenkrich, M., Smith, J. C., Stote, R., Straub, J., Watanabe, M., Wiorkiewicz-Kuczera, J., Yin, D., and Karplus, M. (1998) All-Atom Empirical Potential for Molecular Modeling and Dynamics Studies of Proteins. *J. Phys. Chem. B 102*, 3586–3616.
28. Brunger, A. T., Brooks, C. L., III, and Karplus, M. (1985) Active Site Dynamics of Ribonuclease. *Proc. Natl. Acad. Sci. U.SA. 82*, 8458–8462.
29. Brooks, C. L., and Karplus, M. (1989) Solvent Effects on Protein Motion and Protein Effects on Solvent Motion: Dynamics of the Active Site Region of Lysozyme. *J. Mol. Biol. 208*, 159–181.
30. Ryckaert, J. P., Ciccotti, G., and Berendsen, H. J. C. (1977) Numerical integration of the cartesian equations of motion of a system with constraints: Molecular dynamics of *n*-alkanes. *J. Comput. Phys. 23*, 327–341.
31. Nicholls, A., and Honig, B. (1991) A rapid finite difference algorithm, utilizing successive over-relaxation to solve the Poisson-Boltzmann equation. *J. Comput. Chem. 12*, 435–445.
32. Klapper, I., Hagstrom, R., Fine, R., Sharp, K., and Honig, B. (1986) Focusing of electric fields in the active site of Cu-Zn superoxide dismutase: Effects of ionic strength and amino-acid modification. *Protein 1*, 47–59.
33. Nina, M., Beglov, D., and Roux, B. (1997) Atomic Radii for Continuum Electrostatics Calculations based on Molecular Dynamics Free Energy Simulations. *J. Phys. Chem. B 101*, 5239–5248.
34. Schaefer, M., Sommer, M., and Karplus, M. (1997) pH-Dependent of Protein Stability: Absolute Electrostatic Free Energy Differences between Conformations. *J. Phys. Chem. B 101*, 1663–1683.
35. Cui, Q., Elstner, M., Kaxiras, E., Frauesheim, Th., and Karplus, M. (2001) A QM/MM Implementation of the Self-Consistent Charge Density Functional Tight Binding (SCC-DFTB) Method. *J. Phys. Chem. B 105*, 569–585.
36. Elstner, M., Porezag, D., Jungnickel, G., Elsner, J., Haugk, M., Frauenheim, Th., Suhai, S., and Seifert, G. (1998) Self-Consistent-Charge Density-Functional Tight-Binding Method for Simulation of Complex Materials Properties. *Phys. Rev. B 58*, 7260–7268.
37. Fischer, S., and Karplus, M. (1992) Conjugate Peak Refinement: An Algorithm for Finding Reaction Paths and Accurate Transition States in Systems with Many Degrees of Freedom. *Chem. Phys. Lett. 194*, 252–261.
38. Hu, P., and Zhang, Y. (2006) Catalytic Mechanism and Product Specificity of the Histone Lysine Methyltransferase SET 7/9: An ab initio QM/MM-FE study with Multiple Initial Structures. *J. Am. Chem. Soc. 128*, 1272–1278.
39. Wiberg, K. B. (1968) Application of the Pople-Santry-Segal complete neglect of differential overlap method to the cyclopropylcarbinyl and cyclobutyl cation and to bicyclobutane. *Tetrahedron 24*, 1083–1096.
40. Frisch, M. J., Trucks, G. W., Schlegel, H. B., Scuseria, G. E., Robb, M. A., Cheeseman, J. R., Montgomery, J. A., Jr., Vreven, T., Kudin, K. N., Burant, J. C., Millam, J. M., Iyengar, S. S., Tomasi, J., Barone, V., Mennucci, B., Cossi, M., Scalmani, G., Rega, N., Petersson, G. A., Nakatsuji, H., Hada, M., Ehara, M., Toyota, K., Fukuda, R., Hasegawa, J., Ishida, M., Nakajima, T., Honda, Y., Kitao, O., Nakai, H., Klene, M., Li, X., Knox, J. E., Hratchian, H. P., Cross, J. B., Bakken, V., Adamo, C., Jaramillo, J., Gomperts, R., Stratmann, R. E., Yazyev, O., Austin, A. J., Cammi, R., Pomelli, C., Ochterski, J. W., Ayala, P. Y., Morokuma, K., Voth, G. A., Salvador, P., Dannenberg, J. J., Zakrzewski, V. G., Dapprich, S., Daniels, A. D., Strain, M. C., Farkas, O., Malick, D. K., Rabuck, A. D., Raghavachari, K., Foresman, J. B., Ortiz, J. V., Cui, Q., Baboul, A. G., Clifford, S., Cioslowski, J., Stefanov, B. B., Liu, G., Liashenko, A., Piskorz, P., Komaromi, I., Martin, R. L., Fox, D. J., Keith, T., Al-Laham, M. A., Peng, C. Y., Nanayakkara, A., Challacombe, M., Gill, P. M. W., Johnson, B., Chen, W., Wong, M. W., Gonzalez, C., and Pople, J. A. 2004 *Gaussian*, Gaussian, Inc., Wallingford, CT.
41. McQuarrie, D. A. (1973) *Statistical Thermodynamics*, Harper and Row, New York.
42. Schmidt, M. W., Baldridge, K. K., Boatz, J. A., Elbert, S. T., Gorden, M. S., Jensen, J. H., Koseki, S., Matsunage, N., Nguyen, K. A., Su, S. J., Windus, T. L., Dupuis, M., and Montgomery, J. A. (1993) General atomic and molecular electronic-structure system. *J. Comput. Chem. 14*, 1347–1363.
43. Cui, Q., and Karplus, M. (2001) Triosephosphate Isomerase: A Theoretical Comparison of Alternative Pathways. *J. Am. Chem. Soc. 123*, 2284–2290.
44. Zhang, X.-D., Harrison, D. H. T., and Cui, Q. (2002) The functional specificities of methylglyoxal synthase (MGS) and triosephosphate isomerase (TIM) are not due to stereoelectronic effects: A combined QM/MM analysis. *J. Am. Chem. Soc. 124*, 14871–14878.
45. Takusagawa, F., Fujioba, M., Spies, A., and Schowen, R. L. (1998) S-Adenosylmethionine (AdoMet)-dependent Methyltransferases, in *Comprehensive Biological Catalysis: A Mechanistic Reference* (Sinnott, M., Ed.) pp 1–30, Academic Press, New York.
46. Trievel, R. C., Beach, B. M., Dirk, L. M. A., Houtz, R. L., and Hurley, J. H. (2002) Structure and Catalytic Mechanism of a SET Domain Protein Methyltransferase. *Cell 111*, 91–103.
47. Wang, S., Hu, P., and Zhang, Y. (2007) Ab Initio Quantum Mechanical/Molecular Mechanism Molecular Dynamics Simulations of Enzyme Catalysis: The Case of Histone Lysine Methyltransferase SET7/9. *J. Phys. Chem. B 111*, 3758–3764.
48. Guo, H. B., and Guo, H. (2007) Mechanism of histone methylation catalyzed by protein lysine methyltransferas SET7/9 and origin of product specificty. *Proc. Natl. Acad. Sci. U.S.A. 104*, 8797–8802.

BI702370P